TW5-TVR-AIA

Task Title: ARTICULATED INSPECTION ARM (AIA)

INTRODUCTION

The Articulated Inspection Arm (AIA) project takes place in the Remote Handling (RH) activities for the next step fusion reactor ITER. The aim of this R&D program is mainly to demonstrate the feasibility of close inspection of the Divertor Cassettes and the Vacuum Vessel first wall of a Tokamak with a long reach multi link and limited payload carrier called AIA. We assumed that the AIA robot penetrates the first wall using the 6 penetrations evenly distributed around the machine.

The need to access close to the Vacuum Vessel first wall and the Divertor cassettes had been identified. This is required when considering inspection with other processes as camera or leak detection.

The work performed under the EFDA-CSU Workprogramme includes the design, manufacture and testing of an articulated device demonstrator called Articulated Inspection Arm (AIA).
The AIA has to fulfil the following specifications:

- Elevation: +/- 45 ° range,
- Rotation: +/- 90 ° range,
- Robot total length: 7.4 meters,
- Admissible payload: 10 Kg,
- Temperature: 200 °C during baking – 120 °C under working,
- Pressure: 9.7 10^{-6} Pa – Ultra high vacuum.

Therefore a scale one full module with 2 degrees of freedom was manufactured and tested under Tore Supra (TS) requirements (temperature and pressure). The manufacture of the complete AIA robot, the deployer and the storage cask is now achieved. The design of the video process is completed, the procurement and its manufacture is foreseen in the first months of 2007.

2006 ACTIVITIES

PROTOTYPE MODULE ACTIVITIES SUMMARY

2006 was first dedicated to the segment baking tests (200°C). Then, the segment cycling test campaign in air and at room temperature was carried on in CEA-Cadarache facilities to validate the mechanical behaviour and service life of the most stressed module of the whole robot. The successful results enabled to start the whole robot manufacture and procurement.
Succeeding maintenance and expertise operations, a new test campaign in Tore Supra facility ME60 was carried on to fully qualify the robot under vacuum and temperature conditions.

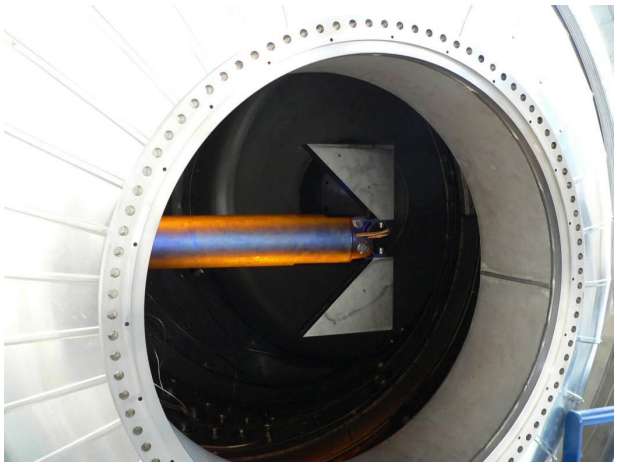

Figure 1: Prototype module test campaign in ME60 facility - March 2007

AIA ROBOT MANUFACTURE

The complete manufacture of the AIA robot ended in autumn 2006 and the whole robot is being assembled in CEA-Fontenay-aux-Roses facilities.

Figure 2: Clevis subassembly

Figure 3: Segment assembly (First segment)

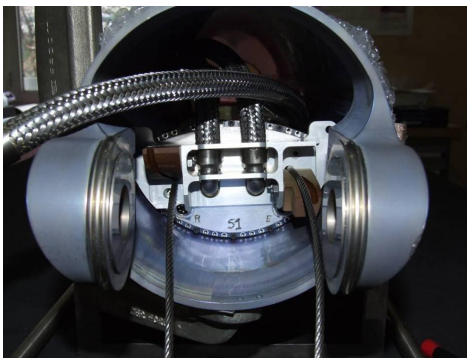

Figure 4: Vue of the rotation box assembled into the tube (First segment)

A demonstration of the AIA behaviour and reliability in real temperature and vacuum Tokamak environment is planned on Tore Supra test facilities.

STORAGE CASK AND DEPLOYER MANUFACTURE

The storage cask is performed to condition the AIA robot before its introduction into the tokamak. This 11 meter stainless steel material structure has to insure the baking phase (200°C) of the AIA robot during several days. It also insures the ultra high vacuum conditioning so it is connected to vacuum pumps and must remain perfectly tight.
The storage cask manufacture is achieved and tests are carried on in CEA-Cadarache facilities.

Figure 5: Storage cask dome welding

The deployer, also called the passive module of the AIA robot, enables to push the AIA robot on its stroke. It is actuated by an electric motor and its control is based on the position sensor signal. This structure is also made in stainless steel material to be compatible with ultra high vacuum constraints.
The deployer manufacture is also achieved and the assembly is being tested in the storage cask in real temperature conditions.

Figure 6: Storage cask, deployer and holding cable chain assembly

VIDEO PROCESS

At this step of the project, the design of the video process is already achieved and the procurement is about to start.

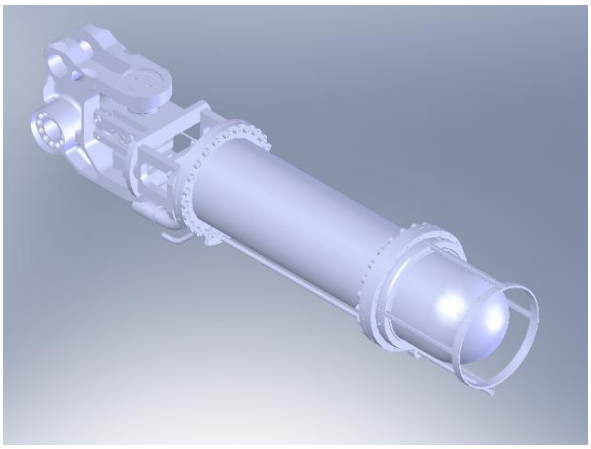

Figure 7: 3D design of the video process

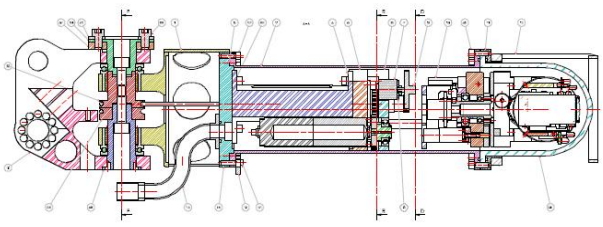

Figure 8: Plan of the video process design

CONCLUSIONS

Integration and tests of the complete AIA robot is planned during the beginning of 2007. The complete integration of the AIA robot on the deployer and storage cask is planned for 2007.

Demonstration of the AIA behaviour and reliability in real temperature and vacuum Tokamak environment is planed on Tore Supra test facilities.

This robotic device gives new perspectives on maintenance and operating activities for a reactor like ITER and aims to enhance operator perception of in-vessel situation.

REFERENCES

- European Fusion Technology Programme
  Task TW0-DTP 1/2,
  Task TW0-DTP 1/4,
  Task TW1-TVA/IVP,
  Task TW2-TVA/IVP,
  Task TW3-TVR/IVV,
  Task TW4-TVR/AIA.

REPORTS AND PUBLICATIONS

CEA/DTSI/SRI/LRM/ 07RT.007-Issue 0
Manufacturing and procurement of AIA last modules, storage cask and video process. Delphine KELLER

TASK LEADER

Jean Pierre FRICONNEAU

DRT/DTSI/SRSI
CEA-Fontenay-aux-Roses
18, route du Panorama – BP6
F-92265 Fontenay-aux-Roses Cedex

Tel. : 33 1 46 54 89 66
Fax : 33 1 46 54 75 80

e-mail : jean-pierre.friconneau@cea.fr

TW5-TVR-RADTOL

Task Title: RADIATION TOLERANCE ASSESSMENT OF STANDARD ELECTRONIC COMPONENTS FOR REMOTE HANDLING

INTRODUCTION

The objective of 2006 activity is the qualification of an embedded electronic module used for digitalising and transferring analog signals coming from an angular position sensor (resolver). This work is connected with previous studies performed between 2003 and 2005.
Initial works investigated the availability of RH components electronic functions applied to the limitation of umbilical wire sizes.
Mock-ups were developed for the most useful sensors, i.e. resolvers and LVDT.
Experiments were done under test conditions as close as possible to the real ITER environment. Results were confident enough to engage in 2005 the prototyping of an electronic 12-bit converter and 16-bit serial multiplexers for a resolver and LVDT (only 8 bits converter).
Unfortunately, the resolver's prototype was unable to deliver correct signals. Scheduling of irradiation by the end of year 2005 saved a short time to enable partial recover of critical functions. Results presented in [1] were used to design with new rules a more efficient prototype and organise a new validation sequence.
The main objectives of the task achieved in 2006 were to consolidate this earlier work by designing a new radiation hardened system (under the same environments) and manufacture it. A second aspect of this work was to evaluate the accuracy of the R/D 12-bits conversion subsystem before and during irradiation, for different angular positions.

2006 ACTIVITIES

The new prototype was delivered by the end of year 2005, taking into account most of the necessary new design rules.

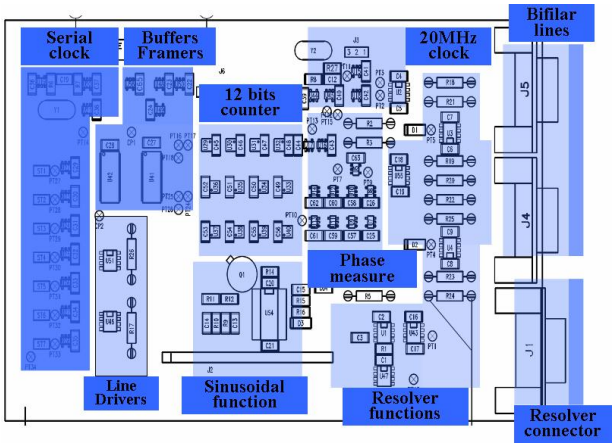

Figure 1: Components routing on PCB

With respect to functional blocks previously presented in [1], figure 1 shows an overall PCB implantation of the various electronic modules used to realise the 12-bit digital converter and 16-bit serial frame transmission.
Each of these functions was controlled in order to evaluate the efficiency of the new design rules for previous deficient modules needed to drive a "BRT" resolver or resolver "ϕ".
The output delivered by the component $A\sin(\omega t + / - \phi)$ was issued from the two input signals $A\sin(\omega t)$ and $A\cos(\omega t)$ where ϕ is the angular position to measure.
This angle was then converted to duration by the phase measure module as shown on figures 2 and 3.

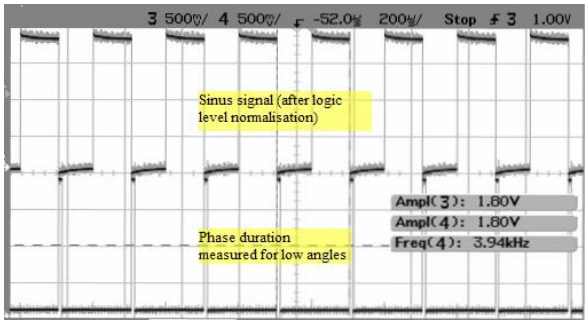

Figure 2: Phase measurement (small angular position)

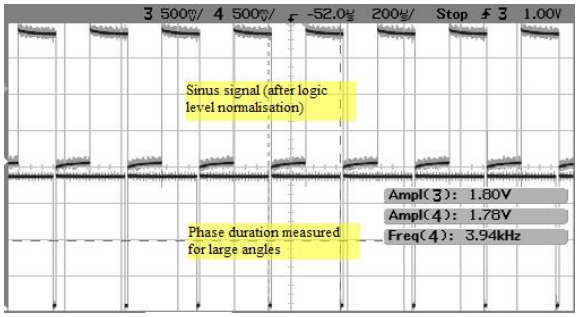

Figure 3: Phase measurement (large angular position)

The phase to duration signal was then sliced into burst of pulses cadenced by the 20MHz clock as shown on figure 4.

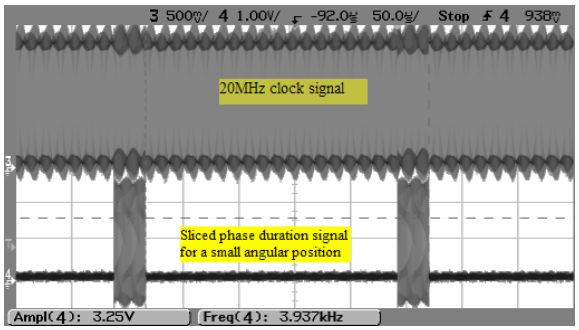

Figure 4: Slicing of phase duration signal

Further control trials were carried out on the prototype with respect to the largest availability of internal functions (12 bits counter, 16 bits frame LVDS signals, …).
Due to the lack of synchronisation between serial clock signals, division of quartz basic oscillation and buffering/framing clock, signal division of resolver basic oscillation was later modified on the new PCB in order to rectify the duration of the first bit of the frame as represented on figures 5 and 6.

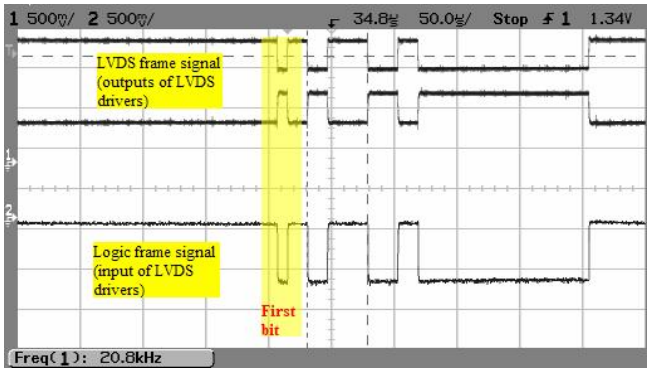

Figure 5: Duration of first bit before rectification

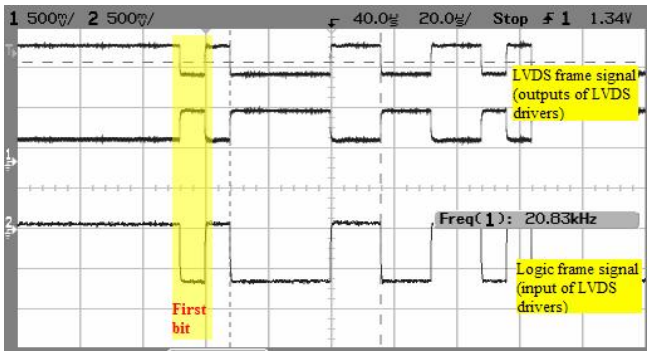

Figure 6: Duration of first bit after rectification

Then, the prototype board was exposed to a radiation field of about 7,5kGy/h during a week in order to reach a total dose of about 800kGy. No on-line tests were conducted during this time.
The post-irradiation measures were done a few days after the end of the irradiation.
No significant problems were reported. Nevertheless, some bits of the frame were affected by an instability mainly induced at the level of the resolver functions.

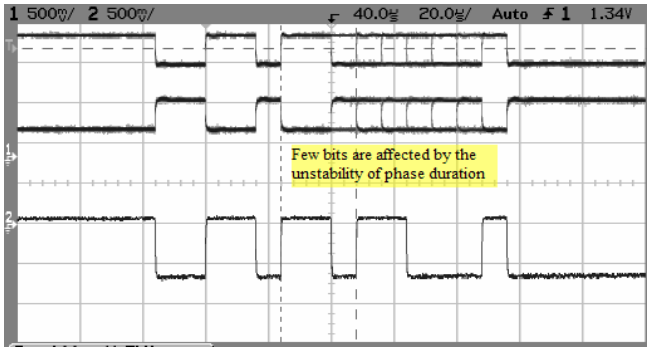

Figure 7: Instability inherent to the phase duration function

The chronogram of figure 7, as well as some recordings for two angular positions, displays the faulty effect of the resolver cable.
In order to take into account a nominal configuration of a long cable between resolver and conditional signal board, it was necessary to use a shielded cable, and this was done for the next step of the study (accuracy measurement during an irradiation process).
Angular position calibration (for the resolver, electronic elements and printed board used) provides, with a accessible degree of accuracy, the necessary link between the angular position being the measurement and the digital position registered and sent into the frame.
Under normal conditions, the angular position is very stable considering the use of correct wires and connections. However, most of the involved elements are sensitive to the harsh environment encountered into radiation fields. For these reasons, the study takes into account some recalibration steps to counterbalance damaging radiation effects.

Set-up design
To perform such on-line control and appreciate the degradation of the overall "smart" sensor, the most common method consists in relying on a simple comparison between the sensor and a previously calibrated sensor.
Due to the uniqueness of the module, it was proposed to compare with a standard industrial angular sensor. The reference resolver HEIDENHAIN ROC 413 13bits SSI output frame was used.
By mounting the tested resolver to the reference and then connecting this combination to a suitable rotation source, it has been possible to move both devices and compare the data.
As shown on figure 8, we developed and automated a set-up using a simple DC motor and equipped with gear wheels to reduce rotation speed at a very low level. The final axe of the gear box allows the connection of the two resolvers and then a common rotation.

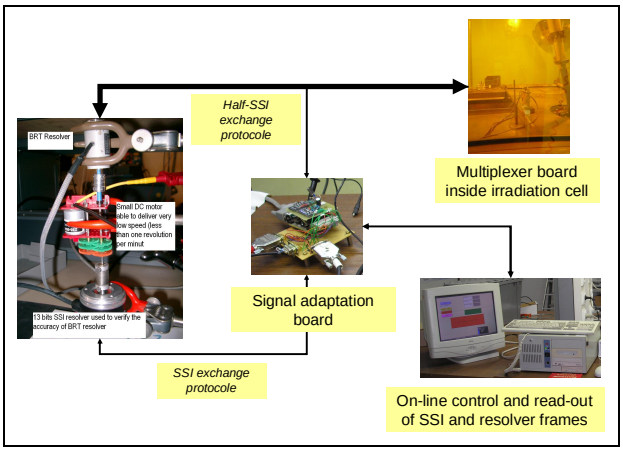

Figure 8: Set-up for accuracy evaluation

Because the multiplex serial link was designed as a pseudo SSI protocol (no clock was delivered by the control system) while the ROC413 disposes of a full SSI one, it was developped an adaptation board. It includes a clock generator, RS485 and LVDS voltages translations to TTL level, compatible with control read-out.

A specific software was written to drive the reading, the recording and the visualization of the digitalised angular positions of both the BRT (through multiplexer board) and ROC413 resolvers.
In addition, other useful information concerning the behaviour of specific electrical parameters was also recorded by an other PC equipment.

On-line laboratory recording
Some laboratory experiments were done just before starting the irradiation. Unfortunately, more significant and exhaustive measurements were not considered due to a limited time schedule.
We observed at room temperature conditions, as reported on figure 9, the behaviour of both ROC413 and BRT resolvers during about 10 hours for one angular position given after having stopped the rotation of the DC motor. The scanning of the two frames was realised every second.
The resulting curve for the recorded BRT data shows a mean value plus a drift of less than 4 points (an equivalent noise of about 2 bits at the level of the prototype board).
The stability measurement gave an approximate value of 4*360/4096 (12 bits) ~= 0,3° for the corresponding angular position.
No fluctuation was seen for the industrial resolver.
This result was an encouraging first step, even if some artefacts partly induced by the scanning mechanism were visible (fully dependant of the operating system used on the control PC, an old Windows version).

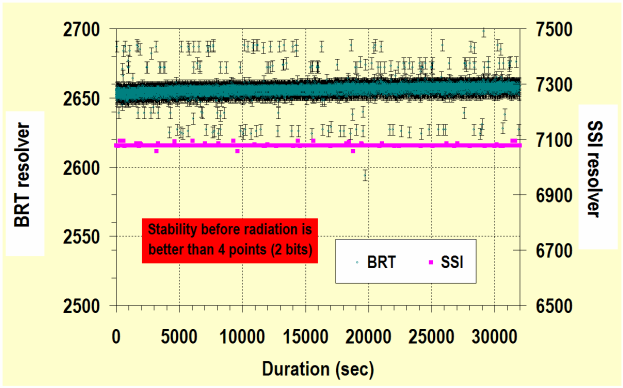

Figure 9: Stability observed for one point during 10 hours

The second preliminary experiment was done with rotation induced by DC motor. The speed was slowed as much as possible with our DC motor and gear box in order to measure the smallest possible angle variations.
The results of this experiment are shown on figure 10. The curves represent BRT resolver = f(SSI resolver) in order to easily compare the expected linear transcription of the angular position to a binary value for both resolvers. In normal conditions, the linearity of the resulting curve must be clearly visible.
The curves showed also this linearity. Globally, the multi revolution of the resolver axes led to a correct repetitiveness of the digital recorded data with a precision of about 3 bits. However, the curve was made up of three distinct elements *(points 5, 6 and 7)*. The curves referenced as *point 5* and *point 7* were obtained for an angular position generating binary position 0 to 12-bits maximum value of the counter. The curve *"point 6"* was unfortunately a consequence of the independence of the frequencies chosen for the clock counter (20MHz) and for the resolver. A full phase of an angular position of 360° needs more than 12-bits to be sliced at 20 MHz. This part of the curve represents the extra counting.
Moreover, the figure highlights some static measures *(points 1)* which were induced at very low speed, the DC motor being unable to assume a regular rotation or even sometimes to move.

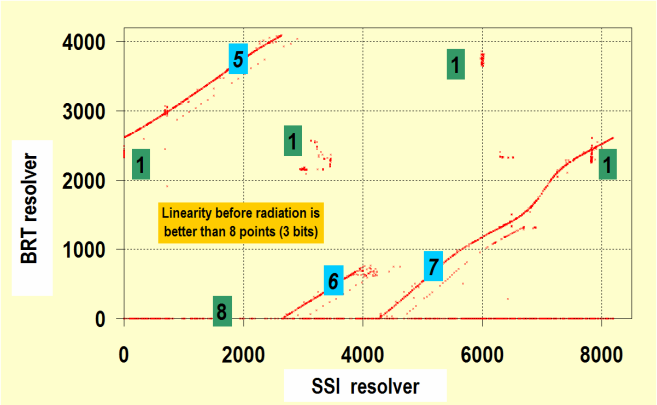

Figure 10: Accuracy observed during multiple full rotations

On-line recording during irradiation
This technique offers the possibility to cover a large inspection range with only one transducer and without any mechanical displacement. For that case, the geometrical requirement related to the maximal available area is respected, that is to say 80 mm from the weld center axis.
Acquisitions were carried out on the prototype inserted inside the cell under γ rays at the dose rate of about 7.9kGy/h during 168 hours, up to a total dose of 130 kGy.
No destruction was resulting of such environment. Nevertheless, some drifts were observed during the first irradiation hours, involving the conversion of the static angular position to duration.
The measurements done with an oscilloscope gave a starting value at about 76µs, followed an hour later by a value of 67 µs. The main components were probably the analog components such as the OPAs. The curves of figure 11 related to this period clearly showed the quick degradation followed by a very slow recovery. After about 18 hours, the last point of the curves, an oscilloscope control gave a value of 67 µs.

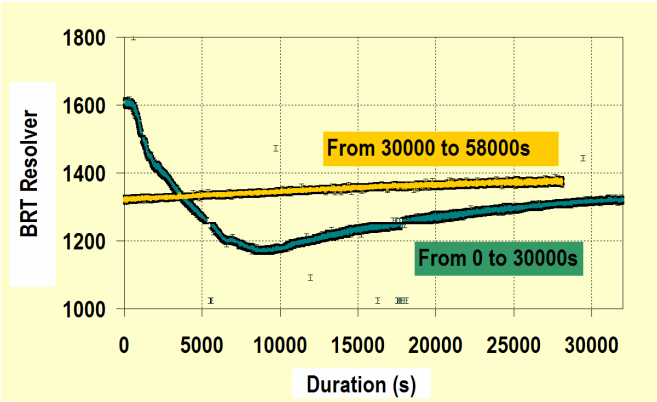

Figure 11: Drifts observed during the first hours under radiation

The next curve, figure 12, shows the accuracy and linearity controls after 0.75MGy total dose. As can be seen, no damage was observed and the good reproducibility of the counting / discounting during these 8 hours was an interesting result. This curve highlighted also an ambiguous behaviour when angular position passed from 360° to 0°C (already seen on figure 10). A bad timing on the signal applied to the clear function of the counter was a reason which has to be taken into account.

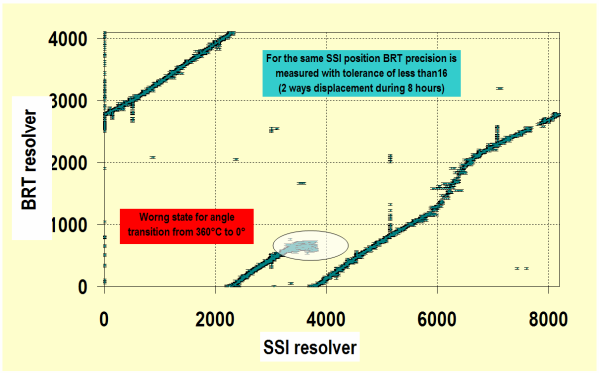

Figure 12: Accuracy and linearity observed after 0.75Mgy

A new static period was established during a two days period between 0.8MGy and 1.2MGy. The stability of the BRT angular conversion was still effective with a precision of less than 3 bits as shown on figure 13. However, an unexpected drift increased the angular conversion to an intermediate value. A continuous decrease was later observed on figure 14. Control of the duration, set at 102µs at the beginning of this observation period, was still at the same value after 1.2MGy.

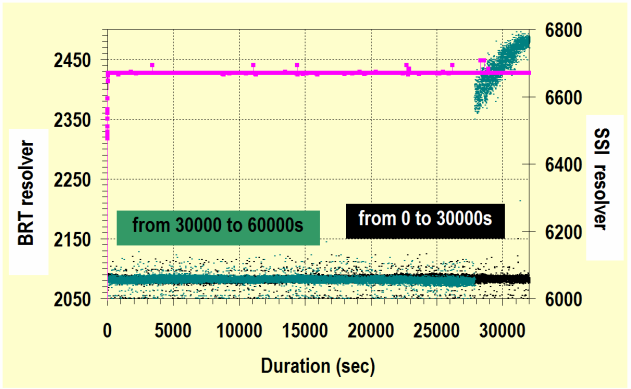

Figure 13 : Static angular position from 0.8MGy to 1MGy

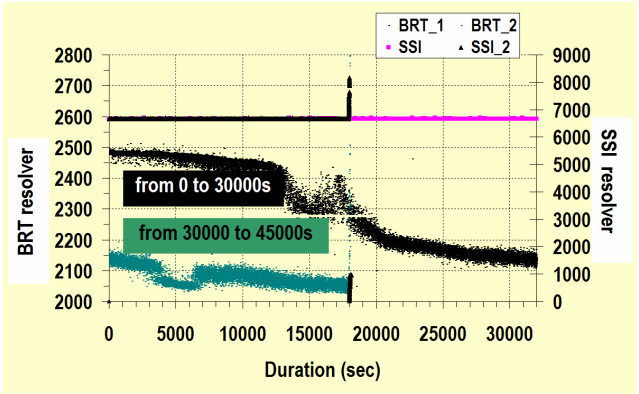

Figure 14 : Static angular position from 1MGy to 1.2MGy

A new angular position was then initiated by rotation of the DC motor. But the BRT instability on the converted frame was still present.
At that radiation level, one possible reason of this erroneous comportment should normally be related to the threshold voltage shift which needs to increase progressively the logic components' power supply in order to be recovered. That was done by changing the logic supply from 1.74V to 1.88V.
This bias condition was kept for the last irradiation period from 1.2MGy to 1.3MGy.
A permanent rotation of the motor was also effective in order to evaluate the accuracy before stopping the experiment. Unfortunately, the action was stopped very quickly. Nevertheless, the accuracy seems correct as represented on figure 15.

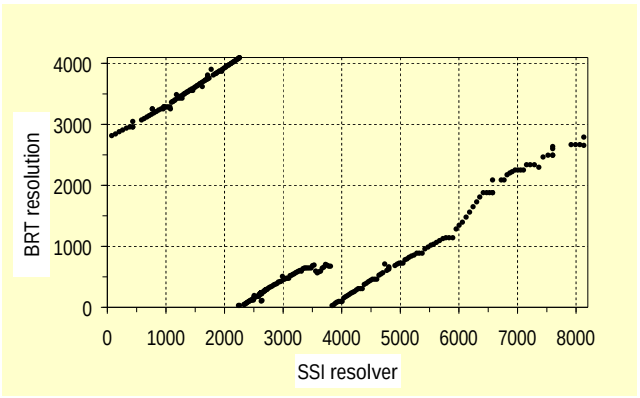

Figure 15: Accuracy at the end of the experiment

Last irradiation period done with a permanent position of the encoders over lighted a correct stability of the converted angular position as shown on Figure 16. However, few moments before end of irradiation period, the very slow degradation of logic threshold was starting to be visible.
The necessary automatic adjustment of logic supply voltage after a certain amount of integrated dose was becoming one of the key functions for electronic embedded in high total dose environment. As seen during previous RADTOL tasks, a permanent excessive voltage could induce erratic behaviors but also and mainly an early ageing not suitable in such severe environmental conditions.

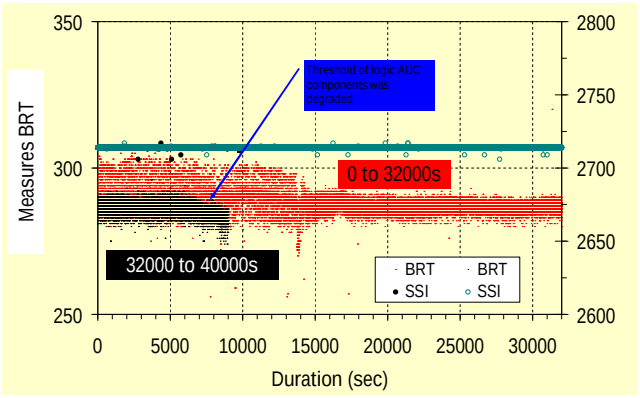

Figure 16: Static angular position from 1.2 to 1.3 MGy

CONCLUSIONS

Further experimental trials have been carried out on the prototype to ensure the accuracy and linearity of the multiplexer conversion module for a BRT resolver.
These acquisitions have shown the validity of this conversion method. However, some radiation effects were still present on a few critical components. Some others were easily recoverable.
Since EFDA indicates that the resolver seems to be calibrated by comparison with another one used as a reference, the validity range of the embedded module was particularly studied.
Some overviews of static angular positions have been seen in terms of stability of the values produced by the multiplexer. Results were interesting
Accuracy has been viewed more partially, mainly under the point of repetitiveness which was correct. The precision of the measures was not evaluated for two reasons: mechanical problems (our DC motor was not efficient at very low speed) and very short radiation periods.

TASK LEADER

Alain GIRAUD

DRT/DTSI/SARC/LFSE
CEA-Saclay
F-91191 Gif-sur-Yvette Cedex

Tel. : 33 1 69 08 64 30
Fax : 33 1 69 08 20 82

e-mail : alain.giraud@cea.fr

TW5-TVR-WHMAN

Task Title: DEVELOPMENT OF A WATER HYDRAULIC MANIPULATOR

INTRODUCTION

Hydraulic technology can provide powerful actuators in small volumes. For that reason hydraulics becomes an interesting technology to build heavy duty manipulators for maintenance operations in space constrained areas.

Due to potential leaks, oil hydraulic can not be used for maintenance operations in ITER. Pure water hydraulics proposes a good alternative to oil and today's developments are focusing on that direction.

To identify areas of improvement, a standard MAESTRO joint was supplied with water. Characterization of the joint was made both from a mechanical and from a control point of view.

2006 ACTIVITIES

TEST RIG

The test rig (see figure 1) is composed of a 135mdaN vane actuator mounted on a manifold providing pressurized water through a type 30-417 Moog servovalve.

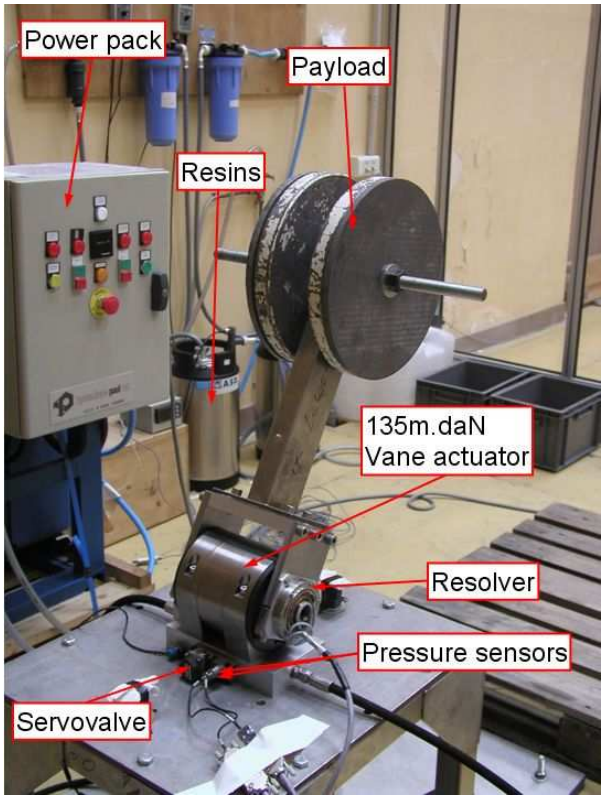

Figure 1: Test rig

Pressure is measured with EPXT pressure sensors of the manufacturer Entran. These are the pressure sensors used in the Maestro hydraulic arm. 4 of them are used to measure:
- The supply pressure.
- The pressure of the return loop.
- Pressure at outlets 1 & 2 of the servovalve.

Position is measured with an Artus-Kollmorgen resolver.
The fluid used in this application is water from the tap demineralized through ion resins cartridges.
Fluid power is supplied by a Danfoss Nessie power unit. Maximum supply pressure is 210 bar with a maximal flow of 45 l/min.

PRELIMINARY TESTS

Identification of the performances of the servovalve was first made on open ports. The flow response of the servovalve to a current input can be modeled by the following polynomial:

$$Q = -0.092 + 1.5708i + 0.0002i^2 - 0.004i^3$$

(Q in L/min and i in mA)

The previous expression of the water flow rate, measured on open ports, doesn't take into account the compressibility of the fluid in the joint chambers and the internal leak rate. For that reason it is not really relevant for use as a control law synthesis. Identification of the flow response of the servovalve to input signals with different frequencies give the results of figure 2.

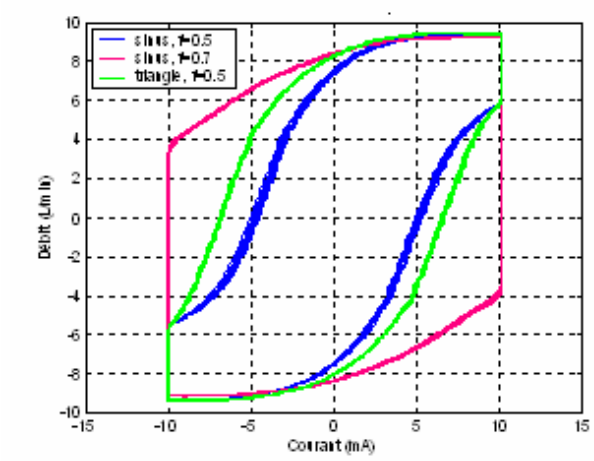

Figure 2: Flow response to current input signals for different frequencies

We see a saturation of the flow rate in both directions to a value close to 9.4 l/min.
According to the joint position, the internal leak rate of the complete assembly varies between 0.8 l/min and 1.3 l/min.
The actuator is able to raise a load of about 156kg at 0.815m, which is close to its real maximal supported torque (1249N.m instead of 1350N.m of the design specification).

PERFORMANCES IN FORCE CONTROL MODE:

The quality of a force control loop highly depends on the quality of the friction and gravity model that are built and used as compensation factors in the control loop. In our case this model takes into account: the arm inertia, the viscous friction coefficient, the dry friction coefficient, an impact factor coefficient of the gravity on the dry friction and an offset torque due to asymmetrical behaviour of the joint.

A theoretical torque is rebuilt according to the mechanical model, from the measurements of the position, the seed and the acceleration, and the identified parameters.
The difference between the measured and rebuilt torques characterizes the accuracy of our identification.
The smaller is the difference, the better the compensation.

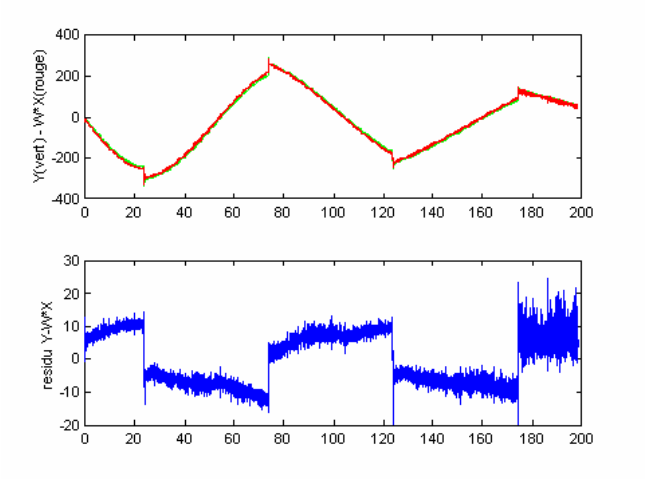

Figure 3: Comparison between real torque and rebuilt torque (red and green) + error graph (blue)

Step (see figure 4a) and ramp tracking response (see figure 4b) of the joint were assessed.

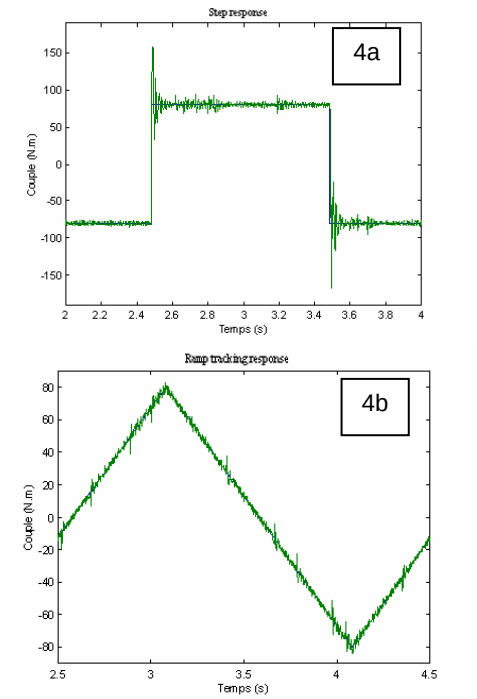

Figure 4: Step and ramp tracking response of the joint

The performances with water are better than the same joint supplied with oil.
The stability of the control loop is guaranteed by the step response and the overshooting that are respectively less than 6ms from -80N.m to 80N.m and 48%. For memory, the overshooting and the time response of the oil device were respectively 82% and about 175ms.

Backdrivability tests provide a good image of the force feedback quality. The joint is moved manually back and forth with a payload. The torque supplied by the operator is evaluated with the pressure sensors and the model and compared to the real torque (see figure 5).

Although a peak value is observed during high speed or high acceleration movements, the behaviour of this joint for remote handling application with force feedback should be very good.

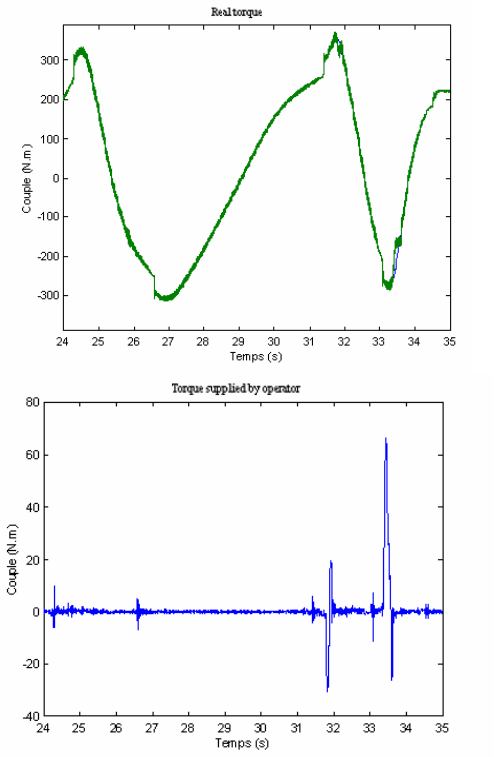

Figure 5: Back drivability tests: real torque (green) + Torque supplied by operator during same period (blue)

Low speed tests are carried out to evaluate the resolution of the position control loop. Due to the friction the position resolution can be simply assimilated to the resolution of the resolver.

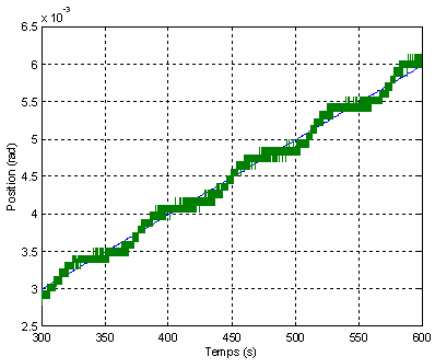

Figure 6: Low speed tests

In force control mode, when gains of the model are not as stiff as they are in a position loop, the resolution in position at the end of the arm is expected to be close to 0.7mm for this axis.

EFFECTS OF TEMPERATURE ON THE BEHAVIOUR

Between 20 and 45°C, high variation of the viscosity of water is observed (close to a factor 2 less). Tests were carried out with water at 22°C and 42°C to evaluate the impact of the temperature on the control scheme. No significant effects were noticed on the control performances. Minor increase of the internal leak rate was noticed.

CONCLUSIONS

Force and position performances of the joint equipped with a water hydraulics flow servovalve are globally similar or better than the one equipped with an oil servovalve. The cylinder manufactured by CYBERNETIX fits the initial requirements and the conception of an entire water hydraulics MAESTRO arm should be successful.
Our efforts will now be concentrated on the evolutions of the design to adapt the joint design to water.
Endurance tests will start to identify all areas of improvement in the mechanical design.

REPORTS AND PUBLICATIONS

DTSI/SRI/LPR/06RT018 Results on qualification of a water-hydraulics joint for force feedback applications

TASK LEADER

Jean Pierre FRICONNEAU

DRT/DTSI/SRI
CEA-Fontenay aux Roses
Boîte Postale 6
F-92265 Fontenay aux Roses cedex

Tel. : 33 1 46 54 89 66
Fax : 33 1 46 54 89 80

e-mail : jean-pierre.friconneau@cea.fr